



Contents lists available at ScienceDirect

Free Radical Biology and Medicine

journal homepage: www.elsevier.com/locate/freeradbiomed

The decylITPP mitochondria-targeting moiety lowers electron transport chain supercomplex levels in primary human skin fibroblasts

Elianne P. Bulthuis^{a,1}, Claudia Einer^{b,1}, Felix Distelmaier^{a,2}, Laszlo Groh^c, Sjenet E. van Emst - de Vries^a, Els van de Westerlo^a, Melissa van de Wal^d, Jori Wagenaars^a, Richard J. Rodenburg^{d,e}, Jan A.M. Smeitink^{d,2}, Niels P. Riksen^c, Peter H.G.M. Willems^a, Merel J.W. Adjobo-Hermans^a, Hans Zischka^{b,f}, Werner J.H. Koopman^{d,g,*}

^a Department of Biochemistry (286), Radboud Institute for Molecular Life Sciences (RIMLS), Radboud Center for Mitochondrial Medicine (RCMM), Radboud University Medical Center (Radboudumc), Nijmegen, the Netherlands

^b Institute of Molecular Toxicology and Pharmacology, Helmholtz Center Munich, German Research Center for Environmental Health, Neuherberg, Germany

^c Department of Internal Medicine (463), Radboud Institute for Molecular Life Sciences (RIMLS), Radboud University Medical Center (Radboudumc), Nijmegen, the Netherlands

^d Department of Pediatrics, Amalia Children's Hospital, Radboud Institute for Molecular Life Sciences (RIMLS), Radboud Center for Mitochondrial Medicine (RCMM), Radboud University Medical Center (Radboudumc), Nijmegen, the Netherlands

^e Translational Metabolic Laboratory (TML), Radboud Center for Mitochondrial Medicine (RCMM), Radboud University Medical Center (Radboudumc), Nijmegen, the Netherlands

^f Institute of Toxicology and Environmental Hygiene, Technical University Munich, School of Medicine, Munich, Germany

^g Department of Human and Animal Physiology, Wageningen University, Wageningen, the Netherlands

ARTICLE INFO

Keywords:

Mitochondrial targeting
Complex I
Trolox
decylITPP
Supercomplexes
Glycolysis

ABSTRACT

Attachment of cargo molecules to lipophilic triphenylphosphonium (TPP⁺) cations is a widely applied strategy for mitochondrial targeting. We previously demonstrated that the vitamin E-derived antioxidant Trolox increases the levels of active mitochondrial complex I (CI), the first complex of the electron transport chain (ETC), in primary human skin fibroblasts (PHSFs) of Leigh Syndrome (LS) patients with isolated CI deficiency. Primed by this finding, we here studied the cellular effects of mitochondria-targeted Trolox (MitoE10), mitochondria-targeted ubiquinone (MitoQ10) and their mitochondria-targeting moiety decylITPP (C₁₀-TPP⁺). Chronic treatment (96 h) with these molecules of PHSFs from a healthy subject and an LS patient with isolated CI deficiency (NDUFS7-V122M mutation) did not greatly affect cell number. Unexpectedly, this treatment reduced CI levels/activity, lowered the amount of ETC supercomplexes, inhibited mitochondrial oxygen consumption, increased extracellular acidification, altered mitochondrial morphology and stimulated hydroethidine oxidation. We conclude that the mitochondria-targeting decylITPP moiety is responsible for the observed effects and advocate that every study employing alkylITPP-mediated mitochondrial targeting should routinely include control experiments with the corresponding alkylITPP moiety.

Abbreviations: α-Toc, α-tocopherol; CI, complex I or NADH: Ubiquinone oxidoreductase; Δψ, mitochondrial membrane potential; ETC, electron transport chain; LS, Leigh syndrome; MD, mitochondrial disease; MIM, mitochondrial inner membrane; MOM, mitochondrial outer membrane; OXPHOS, oxidative phosphorylation; PHSF, primary human skin fibroblast; ROS, reactive oxygen species; SC, supercomplex; TPMP, methyltriphenylphosphonium cation; TPP, triphenylphosphonium cation.

* Corresponding author. Department of Pediatrics, Amalia Children's Hospital, Radboud Institute for Molecular Life Sciences (RIMLS), Radboud Center for Mitochondrial Medicine (RCMM), Radboud University Medical Centre (Radboudumc), P.O. Box 9101, NL-6500 HB, Nijmegen, the Netherlands.

E-mail address: Werner.Koopman@radboudumc.nl (W.J.H. Koopman).

¹ These authors equally share the first authorship.

² **Current address:** FD: Department of General Pediatrics, Neonatology and Pediatric Cardiology, University Children's Hospital Düsseldorf, Heinrich Heine University, Düsseldorf, Germany. JAMS: Khondrion B.V., Nijmegen, The Netherlands.

<https://doi.org/10.1016/j.freeradbiomed.2022.06.011>

Received 16 April 2022; Received in revised form 16 May 2022; Accepted 9 June 2022

Available online 17 June 2022

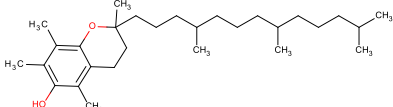
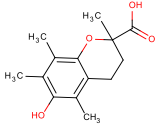
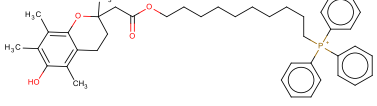
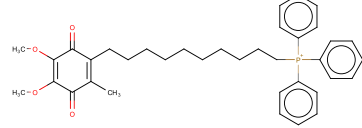
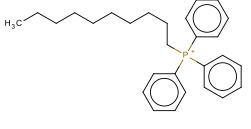
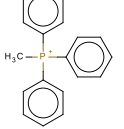
0891-5849/© 2022 The Authors. Published by Elsevier Inc. This is an open access article under the CC BY license (<http://creativecommons.org/licenses/by/4.0/>).

1. Introduction

Mitochondria are among the main producers of cellular ATP and their dysfunction has been implicated in a large variety of human disorders including rare mitochondrial diseases (MDs [1]). Proper mitochondrial function requires the action of the four complexes (CI–CIV) of the electron transport chain (ETC). Together with complex V (CV or F₀F₁-ATPase) this chain constitutes the mitochondrial oxidative phosphorylation (OXPHOS) system, which generates ATP and is embedded in the mitochondrial inner membrane (MIM). Functionally, the ETC sustains an electrochemical proton gradient across the MIM by expelling protons (H⁺) from the mitochondrial matrix. This gradient is associated with a more alkaline matrix pH and an inside-negative MIM electrical potential ($\Delta\psi$). The ETC has been identified as a source of reactive oxygen species (ROS), in particular during mitochondrial dysfunction, and analysis of cells from MD patients revealed increased ROS levels that potentially play a pathophysiological role [2–6]. This suggests that antioxidant treatment might be of therapeutic relevance for MD patients. However, evidence was provided that such a treatment is only (transiently) effective in a limited number of cases [7,8]. Although these observations might relate to the clinical study design [9], they also raise doubts about the therapeutic value of lowering increased ROS levels by exogenous antioxidants in human pathologies [10,11,12].

Mechanistically, it is likely that the different antioxidant effects (or lack thereof) in MD cell models and “real” patients relates to: (a) the type, reactivity, range-of-action, site of generation and physicochemical properties of the ROS, (b) the localization, concentration, specificity, metabolism, degradation and regeneration of the employed antioxidant, (c) the used cell model and culture conditions, and (d) the fact that ROS play dual roles as damaging and signaling molecules [13,14]. In this context, antioxidants can also display pro-oxidant properties, for instance when applied at (too) high concentrations [15]. Given the proposed role of ROS during mitochondrial dysfunction, substantial efforts were made to address some of the above concerns by the development of mitochondria-targeted antioxidants [14,16]. A widely used strategy involves attaching the antioxidant of choice (“cargo”) to a lipophilic triphenylphosphonium (TPP⁺) cation by an alkyl linker [14, 17]. These lipophilic cations distribute themselves across biological membranes according to the Nernst equation in a manner dependent on the plasma membrane potential (ΔV), $\Delta\psi$, temperature, and cation lipophilicity [14,16,18–20]. Alkyltriphenylphosphonium cations enter the mitochondrial matrix by first binding to the MIM outer surface, after which they flip across the core of the phospholipid bilayer and bind to the MIM inner surface [21]. The extent of MIM-binding and depth of MIM side chain penetration increases as a function of the length and hydrophobicity of the alkyl linker [18–22]. Initiating the current study,

Table 1
Molecule structures and lipophilicity.

Name	Structure	Lipophilicity	
		LogP [%]	XLogP3-AA ^{&}
α -Toc		12.2	10.7
Trolox		3.0 ± 0.3	2.8
MitoE10		~2760	ND
MitoQ10		2760 ± 220	9.4
DecylTPP		5000 ± 330	9.1
TPMP		0.35 ± 0.02 2.3 ± 0.2	3.4

[%]LogP = Octanol/water partition coefficient. These values were taken from the literature [21,55,62–67]. The lipophilicity of MitoE10 was similar to that of MitoQ10 (M.P. Murphy, MRC Mitochondrial Biology Unit, University of Cambridge, UK; personal observation).

[&]XLogP3-AA (version 3.0), an atom-additive method that calculates log P by adding up contributions from each atom in the given molecule. These values were taken from PubChem (pubchem.ncbi.nlm.nih.gov/): α -Toc (PubChemCID = 14985); Trolox (PubChemCID = 40634), MitoQ10 (PubChemCID = 1138833); DecylTPP (PubChemCID = 3084562); TPMP (PubChemCID = 74506). Abbreviations: α -Toc, alpha-tocopherol (vitamin E); DecylTPP, decyltriphenylphosphonium; ND, not determined (*i.e.* information not in PubChem); TPMP, triphenylmethylphosphonium.

we previously evaluated the effect of the antioxidant Trolox, a water-soluble α -tocopherol (α -Toc) derivative (Table 1), in primary human skin fibroblast (PHSFs) from an MD patient (P5175) with Leigh Syndrome (LS [23]). These cells harbor a mutation (V122M) in the *NDUFS7* gene encoding a structural CI subunit [24]. It was found that chronic (96 h) Trolox treatment lowered ROS levels and increased the amounts of active CI holocomplex in P5175 cells. To evaluate the potential applicability of mitochondria-targeted antioxidants for mitigation of mitochondrial dysfunction at the cellular level, we here analyzed how the mitochondria-targeted Trolox variant MitoE10 affected bioenergetics in healthy (CT5120) and LS patient (P5175) PHSFs. For comparison, we also studied mitochondria-targeted ubiquinone (MitoQ10) and two mitochondria-targeting moieties decylTPP and TPMP (Table 1). Unexpectedly, we observed that MitoE10, MitoQ10 and decylTPP reduced CI holocomplex levels/activity and the amount of ETC supercomplexes, thereby inducing mitochondrial functional impairment. This strongly suggests that in our cell model the mitochondria-targeting decylTPP moiety is responsible for the observed effects of MitoE10 and MitoQ10.

2. Materials and methods

2.1. Cell culture

Primary human skin fibroblasts (PHSFs) were obtained from a healthy individual (CT5120) and a Leigh syndrome (LS) patient (P5175) with isolated mitochondrial complex I (CI) deficiency (www.omim.org; OMIM 252010). Biopsies were performed following informed (parental) consent and according to the relevant Institutional Review Boards. The P5175 cell line displayed an isolated CI deficiency due to a mutation in the *NDUFS7* gene (G364A; V122M), encoding a CI structural subunit as described previously [24]. The CT5120 and P5175 cell lines were previously characterized at the genetic, biochemical and cellular level (see Supplement). PHSFs were cultured in Medium 199 (M199; #22340–087; Invitrogen, Breda, The Netherlands) in a humidified atmosphere (95% air, 5% CO₂) at 37 °C. The M199 medium contained Earle's salts, 25 mM HEPES, 5.5 mM D-glucose, 0.7 mM L-glutamine, 10% (v/v) fetal calf serum (#10270; Gibco), and 100 IU/ml penicillin/streptomycin (#15140–056; Gibco).

2.2. Analysis of cell number, oxygen consumption rate (OCR) and extracellular acidification rate (ECAR)

Cell number was determined using crystal violet staining. OCR and ECAR analyses were performed using a Seahorse® XFe96 analyzer (Agilent, Santa Clara, CA, USA). Details are provided in the Supplement.

2.3. Measurement of mitochondrial TMRM intensity, mitochondrial size and hydroethidine oxidation

Cells were stained with the fluorescent cation TMRM (tetramethylrhodamine methyl ester) and visualized using fluorescence microscopy. Mitochondrial TMRM intensity and morphology parameters were quantified using an automated method. For hydroethidine (HET) analysis, live-cell HET-oxidation was quantified using fluorescence microscopy. Details are provided in the Supplement.

2.4. Blue-native polyacrylamide gel electrophoresis

BN-PAGE and in-gel activity (IGA) analysis was performed using mitochondria-enriched fractions as described in the Supplement.

2.5. Fluorescence polarization measurements of membrane fluidity in isolated rat liver mitochondria

Mitochondrial membrane fluidity analysis was performed using fluorescence polarization measurements of DPH (1,6-diphenylhexatriene) and TMA-DPH (trimethylammonium 1,6-diphenylhexatriene) as described in the Supplement.

2.6. Data analysis

Molecule structures were generated using MarvinSketch 6.1.3 software (ChemAxon Ltd., Budapest, Hungary). Image analysis was performed using Image Pro Plus software (Media Cybernetics, Inc., Bethesda, MD, USA) and Metamorph software (Molecular Devices Corporation, Downingtown, PA, USA). Curve fitting and statistical analyses were performed using Origin Pro software (Originlab Corp., Northampton, MA, USA). Unless stated otherwise, data is presented as the mean \pm SEM (standard error of the mean) and a two-population unpaired Student's t-test was used for statistical analysis.

3. Results

Primed by our previous results with the α -Toc derivative Trolox (see Introduction), we here aimed to obtain insight into how mitochondria-targeted Trolox (MitoE10) impacted on primary human skin fibroblasts (PHSFs). Based upon our previous research (see Supplementary Materials and Methods), a “typical” control (CT5120) and CI-deficient cell line (P5175) were selected. For comparison, the effects of mitochondria-targeted ubiquinone (MitoQ10), the mitochondria-targeting moiety of MitoE10 and MitoQ10 (decylTPP or C₁₀-TPP⁺), and the decylTPP headgroup (TPMP or C₁-TPP⁺) were also analyzed (Table 1).

3.1. Effect of MitoE10, MitoQ10, decylTPP and TPMP on cell number

As a reference, PHSFs were cultured in the presence of increasing concentrations of Trolox for 96 h. This treatment induced a minor decrease in P5175 cell number of ~20% relative to the vehicle-treated condition (Fig. 1; “a”). No significant reduction in cell number was observed for CT5120 cells. Of note, the used maximal Trolox concentration (500 μ M) as well as the incubation time (96 h) were identical to those applied in our previous Trolox studies with these cell lines [23,25]. The latter studies demonstrated that this treatment regimen increased the amount of active CI holocomplex. AlkylTPP-based compounds can display cytotoxic effects at high (μ M) concentrations [26–33]. Therefore, given their Nernstian accumulation in mitochondria and to maintain compatible with our previous MitoQ10 studies in CT5120 cells [25, 34], the impact of MitoE10, MitoQ10, decylTPP and TPMP on cell number was studied using nanomolar concentrations. This revealed that DecylTPP and TPMP did not affect cell number (Fig. 1), whereas MitoE10 and MitoQ10 lowered this parameter by 20–30% at 100 nM concentration. P5175 cells displayed a reduced cell number relative to CT5120 cells at 50 nM MitoE10 (Fig. 1; “b”). These results demonstrate that 96 h treatment with up to 100 nM of decylTPP or TPMP does not affect cell number, whereas 100 nM MitoE10 or MitoQ10 slightly but similarly lower this parameter in CT5120 and P5175 cells.

3.2. Effect of MitoE10, MitoQ10, decylTPP and TPMP on the levels and activity of CI and CII holocomplexes

Given the fact that Trolox increased the amount of active CI holocomplex in our previous studies, we next investigated whether MitoE10, MitoQ10, decylTPP and TPMP (100 nM; 96 h) affected the protein level (“WB-CI”) and in-gel activity (“IGA-CI”) of the CI holocomplex, as well as CII holocomplex levels (“WB-CII”). For this purpose, we combined BN-PAGE and Western blot analysis (Fig. 2A and B).

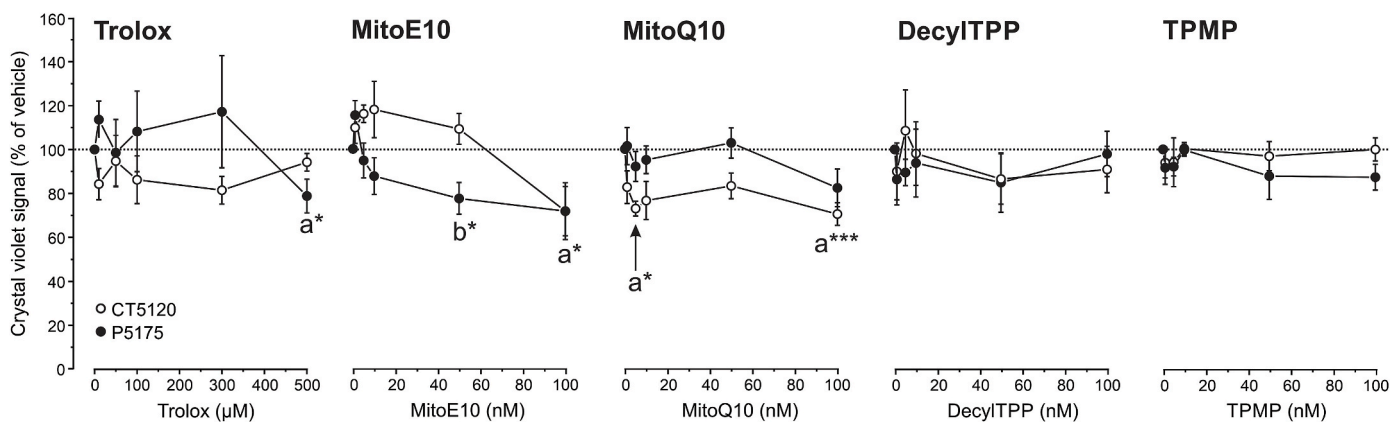


Fig. 1. Effect of Trolox, MitoE10, MitoQ10, decylTPP and TPMP on cell number. PHSFs from a healthy individual (CT5120) and an LS patient (P5175) were cultured in the presence of increasing concentrations of Trolox, MitoE10, MitoQ10, decylTPP and TPMP. Cell number was assessed by crystal violet staining after 96 h. Each data point reflects 3 independent experiments. All data was expressed as percentage of the zero (concentration) condition measured on the same day. Significant differences with the vehicle-treated condition (condition “a”) or CT5120 cell line (condition “b”) are marked by: *($p < 0.05$) and ***($p < 0.001$).

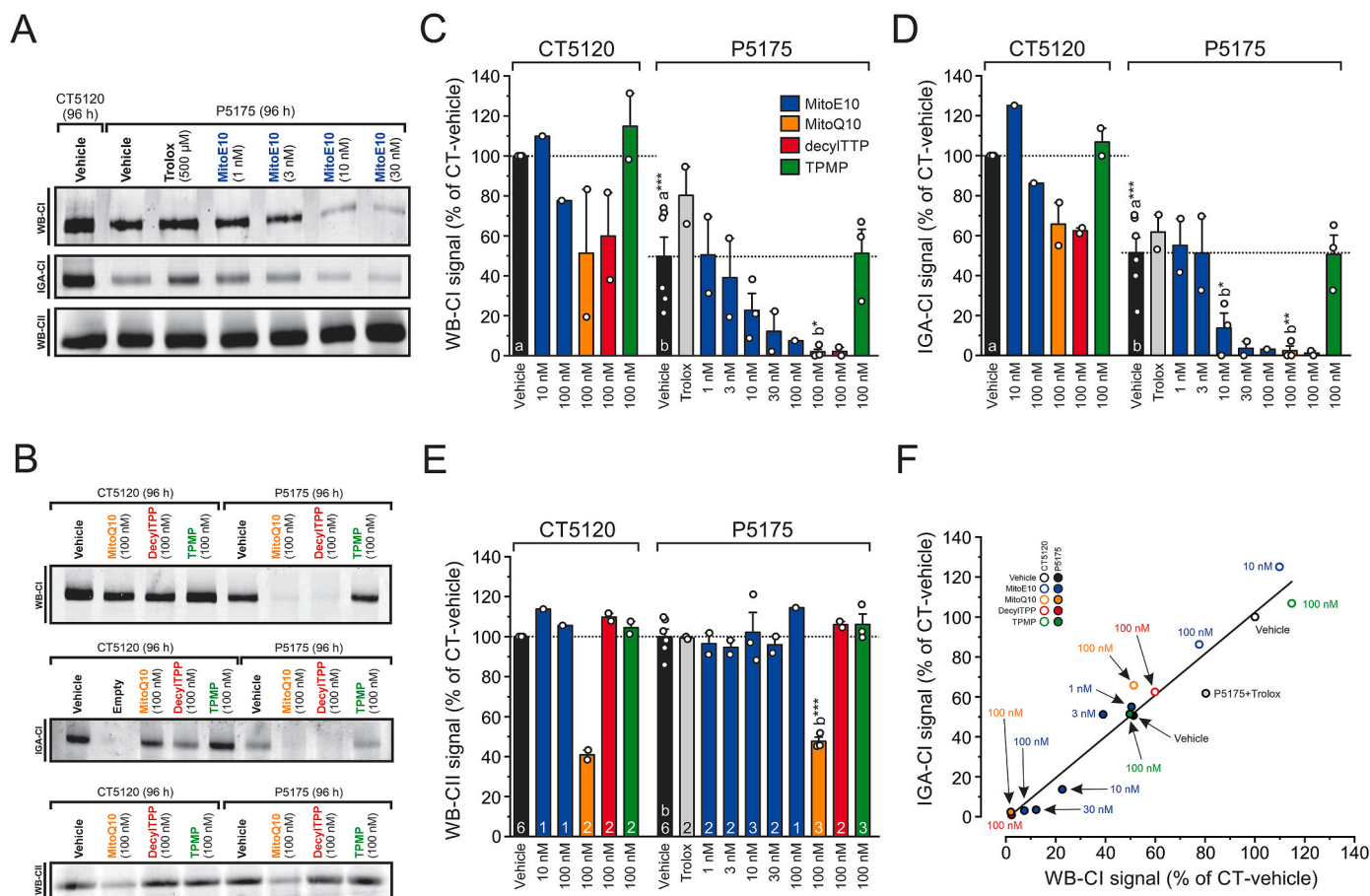


Fig. 2. Effect of MitoE10, MitoQ10, decylTPP and TPMP on the protein levels of mitochondrial holocomplex I and II. (A) PHSFs from an LS patient (P5175) were cultured in the presence of increasing concentrations of MitoE10 for 96 h. PHSFs from a healthy individual (CT5120) and Trolox treatment (500 μ M) were included as controls. Blue-native polyacrylamide gel electrophoresis (BN-PAGE) and Western blot (WB) analysis were applied to visualize mitochondrial complex I (WB-CI) and complex II (WB-CII) holocomplexes. In-gel activity analysis was used to visualize complex I activity (IGA-CI). (B) Similar to panel A but now for CT5120 and P5175 cells cultured in the presence of 100 nM MitoQ10, decylTPP or TPMP. (C) Quantification of the WB-CI bands in panel A–B (including additional experimental data presented in [Supplementary Fig. S1](#)). Symbols indicate independent experiments, the number of which is provided in panel E. Error bars reflect the standard deviation of the data. (D) Same as panel C, but now for the IGA-CI signal. (E) Same as panel C, but now for the WB-CII signal. (F) Correlation between the data in panel C and D. The line represents a linear fit. The blots/gels in panel A–B were contrast-inverted and -optimized for visualization purposes. The original blots/gels are presented in [Supplementary Figs. S7A–B](#). Statistically significant differences relative to the indicated columns (a,b) are marked by: *($p < 0.05$), **($p < 0.01$) and ***($p < 0.001$). (For interpretation of the references to color in this figure legend, the reader is referred to the Web version of this article.)

Control experiments confirmed that Trolox treatment increased WB-CI and IGA-CI in P5175 cells (Fig. 2A-C-D). Unexpectedly, MitoE10 dose-dependently reduced these signals with IC50 values of 6.4 ± 0.96 nM (WB-CI) and 7.0 ± 0.75 nM (IGA). Similarly, MitoQ10 and decylTPP greatly reduced the WB-CI and IGA-CI signal in P5175 cells, whereas these parameters were reduced to a lesser extent in CT5120 cells (Fig. 2B-C-D). TPMP did not induce major alterations in WB-CI or IGA-CI signal in P5175 and CT5120 cells (Fig. 2B-C-D). With respect to WB-CII, Trolox and MitoE10 did not affect this parameter in P5175 cells (Fig. 2A-E). DecylTPP and TPMP also displayed no effect on WB-CII in CT5120 and P5175 cells, whereas MitoQ10 treatment greatly reduced this signal (Fig. 2B-E). Regression analysis demonstrated that the WB-CI and IGA-CI signals were linearly ($y = x$) correlated (Fig. 2F; $p < 0.0001$; $R = 0.973$; intercept = -1.26 ± 4.14 (SE); slope = 1.04 ± 0.0655 (SE)). This strongly suggests that MitoE10, MitoQ10 and decylTPP reduce catalytic CI activity (V_{max}) by lowering the protein levels of the CI holocomplex [25,34]. This conclusion was supported by enzymatic assays (Supplementary Fig. S2) demonstrating that maximal CI activity was reduced by MitoQ10 and decylTPP (but not by TPMP), whereas CII activity was reduced by MitoQ10 (but not by decylTPP and TPMP). Importantly, short-term treatment with MitoQ10, decylTPP or TPMP (100 nM; 30 min) did not affect WB-CI, IGA-CI and WB-CII signals in CT5120 cells (Supplementary Fig. S3A). This suggests that these compounds neither display acute effects on CI and CII holocomplex levels nor affect the isolation yield of these holocomplexes in our experimental conditions. Taken together, our results demonstrate that (in sharp contrast to Trolox and TPMP), MitoE10, MitoQ10 and decylTPP reduce CI levels/activity, particularly in P5175 cells. Additionally, they suggest that MitoQ10 also lowers CII levels.

3.3. Effect of MitoE10, MitoQ10, decylTPP and TPMP on the levels and activity of ETC supercomplexes

CI assembles with ETC complexes III (CIII) and IV (CIV) into supercomplexes of variable stoichiometry [35–39]. Therefore, we next applied BN-PAGE and Western blot analysis of CI (WB-CI), CII (WB-CII) and CIII (WB-CIII) to determine if MitoE10, MitoQ10, decylTPP and TPMP altered supercomplex levels. Five immunoreactive bands were detected in CT5120 cells (Fig. 3A). These bands represented (Supplementary Fig. S4A): (1) the “free” CI monomer (CI-mon; band a), (2) the “free” CIII dimer (CIII-dim; band b), (3) the CI-CIII₂ supercomplex (band c), (4) the CI-CIII₂-CIV supercomplex (band d), and (5) a supercomplex of higher molecular weight (HMW) displaying CI and CIII immunoreactivity (band e). In untreated, vehicle-treated and TPMP-treated CT5120 and P5175 cells, CI and CIII immunoreactivity was primarily associated with CI-CIII₂ (band c) and CI-CIII₂-CIV (band d). The HMW supercomplex (band e) and CI-mon (band a) were occasionally detected in CT5120 cells but not in P5175 cells (Fig. 3A and Supplementary Figs. S4A–B). Further analyses of CT5120 and P5175 cells revealed that treatment (96 h; 100 nM) with MitoE10, MitoQ10 and decylTPP (but not TPMP) reduced supercomplex levels and increased CIII-dim levels (Fig. 3A and B). Compatible with our other results (Fig. 2C-D-F; Supplementary Figs. S2A–B), MitoE10, MitoQ10 and decylTPP reduced supercomplex levels to a lower value in P5175 than in CT5120 cells. Supporting our data in Fig. 2E and Supplementary Fig. S2C, MitoQ10 reduced WB-CII signals in CT5120 and P5175 cells (Fig. 3A and B). Collectively, these results demonstrate that in our cell model: (1) CI and CIII are primarily localized within ETC supercomplexes, (2) treatment with MitoE10, MitoQ10 and decylTPP reduces the levels of these ETC supercomplexes, and (3) MitoE10, MitoQ10 and decylTPP increase the levels of “free” CIII dimers.

3.4. Effect of MitoE10, MitoQ10, decylTPP and TPMP on cellular oxygen consumption and extracellular acidification rate

Decreased incorporation of CI into ETC supercomplexes was

previously linked to impairment of mitochondrial oxygen consumption [38]. Analysis of cellular oxygen consumption (OCR) and extracellular acidification rate (ECAR) revealed that vehicle-treated CT5120 cells displayed a higher routine (basal) and maximal OCR (and a lower routine ECAR) than vehicle-treated P5175 cells (Fig. 4). This indicates that, relative to CT5120 cells, P5175 cells exhibit a reduced mitochondria-mediated ATP production and potentially increased glycolysis-mediated ATP production [40]. These changes are compatible with their CI-deficient state [41,42]. Treatment with MitoE10, MitoQ10 or decylTPP (100 nM; 96 h) reduced routine/maximal OCR and increased routine ECAR in CT5120 and P5175 cells (Fig. 4C-D-E). These effects were either absent or much less pronounced in TPMP-treated cells. Supporting the above results (Fig. 2; Fig. 3; Supplementary Figs. S2A–B), MitoE10, MitoQ10 and decylTPP reduced routine/maximal OCR to a greater extent in P5175 cells than in CT5120 cells, whereas these compounds similarly stimulated routine ECAR in these cell lines (Fig. 4C-D-E; Supplementary Fig. S5). These results demonstrate that MitoE10, MitoQ10 and decylTPP decrease routine OCR and increase routine ECAR. The latter potentially suggests that glycolysis is activated in both cell lines [40,43].

3.5. Effect of MitoE10, MitoQ10, decylTPP and TPMP on mitochondrial TMRM accumulation and mitochondrial morphology parameters

Given the impact of MitoE10, MitoQ10 and decylTPP on CI holocomplex levels, ETC supercomplexes and OCR, we next determined whether $\Delta\psi$ was affected. Since supercomplex disassembly can be paralleled by changes in overall mitochondrial structure [44], we also analyzed mitochondrial morphology parameters. To this end, cells were stained with the mitochondria-accumulating fluorescent cation TMRM (Fig. 5A) and analyzed using a live-cell microscopy strategy previously validated for PHSFs (see Supplementary Materials and Methods). In agreement with our previous studies [45], mitochondria in P5175 cells accumulated less TMRM than in CT5120 cells (Fig. 5B; left panel; black bars), suggesting that $\Delta\psi$ is less negative in P5175 cells. Treatment (100 nM; 96 h) with MitoE10, MitoQ10 and decylTPP (but not TPMP) reduced mitochondrial TMRM accumulation to a similar level in CT5120 and P5175 cells (Fig. 5B; left panel; colorized bars). However, mitochondria still accumulated TMRM under these conditions (Fig. 5A), suggesting that $\Delta\psi$ is less negative but not fully dissipated. Given their extremely flat morphology, various mitochondrial morphological parameters can be quantified from epifluorescence images of TMRM-stained PHSFs [46]. The area of individual TMRM-positive objects (Am ; a measure of mitochondrial size) appeared reduced in cells treated with MitoE10, MitoQ10 and decylTPP but not affected by TPMP (Fig. 5B; right panel). Similarly, the number of mitochondrial objects per cell (Nc) and mitochondrial mass (Mm) appeared reduced in MitoE10- and decylTPP-treated cells, but not in MitoQ10- and TPMP-treated cells (Fig. 5C). Collectively, these results suggest that MitoE10, MitoQ10 and decylTPP partially depolarize $\Delta\psi$ and induce minor aberrations in mitochondrial morphology.

3.6. Effect of MitoE10, MitoQ10, decylTPP and TPMP on the levels of hydroethidine-oxidizing reactive oxygen species

Disruption of the CI-CIII₂ supercomplex was paralleled by increased mitochondrial ROS production [37]. Therefore, we next analyzed the levels of hydroethidine (HET)-oxidizing ROS in cells treated with 10 or 100 nM (96 h) of MitoE10, MitoQ10, decylTPP and TPMP (Fig. 6). Importantly, HET oxidation involves the formation of cationic fluorescent products, which accumulate in the mitochondrial matrix and nucleus. This means that the distribution of these products is $\Delta\psi$ -dependent and fluorescence quantification in both compartments is required for proper analysis [2,34,47]. It was found that mitochondrial and nuclear fluorescence signals displayed a linear correlation in CT5120 (Fig. 6A; $R = 0.93$; $p < 0.0001$; slope = 1.46 ± 0.061 (SE)) and

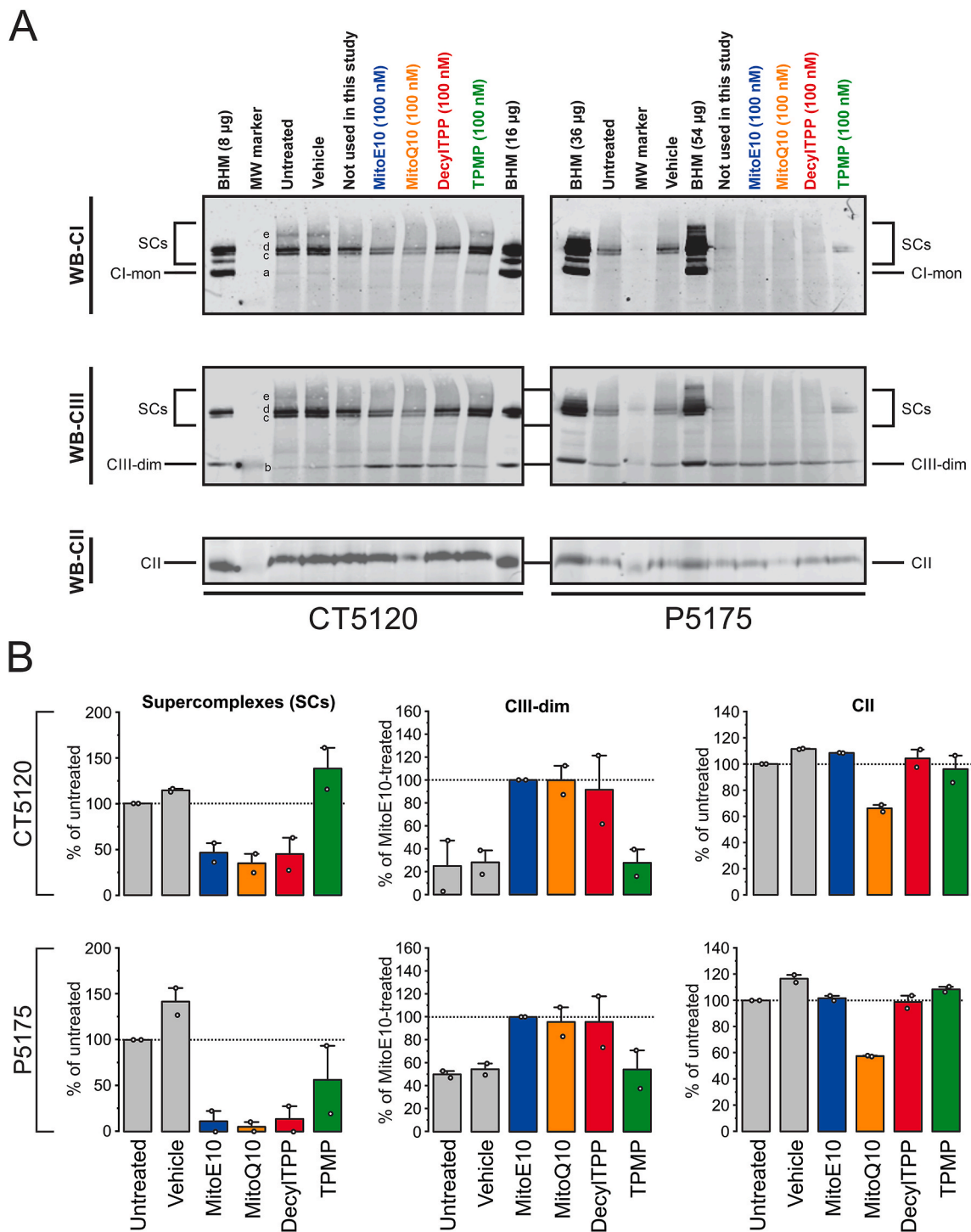


Fig. 3. Effect of MitoE10, MitoQ10, decylTPP and TPMP on ETC supercomplexes. (A) PHSFs from a healthy individual (CT5120) and an LS patient (P5175) were cultured for 96 h in the presence of 100 nM MitoE10, MitoQ10, decylTPP and TPMP. Bovine heart mitochondria (BHM) samples were included as a reference. Blue-native polyacrylamide gel electrophoresis (BN-PAGE) and Western blot (WB) analysis were applied to visualize mitochondrial complex I (WB-CI), complex II (WB-CII) and complex III (WB-CIII). Super-positioning of the WB-CI and WB-CIII signals is provided in [Supplementary Fig. S4A](#). Individual bands correspond to the “free” CI monomer (CI-mon; band a), the “free” CIII dimer (CIII-dim; band b), the CI-CIII₂ supercomplex (band c), the CI-CIII₂-CIV supercomplex (band d) and a higher molecular weight (HMW) supercomplex (band e). (B) Quantification of the bands in panel A (including data from an additional experiment presented in [Supplementary Fig. S4B](#)). Given their close vicinity band c, d and e were quantified simultaneously as supercomplexes (SCs). Symbols indicate independent experiments. Error bars reflect the standard deviation of the data. The blots in panel A were contrast-inverted and -optimized for visualization purposes. Original blots were used for quantification and are presented in [Supplementary Figs. S4A and S4B](#) and S7C. (For interpretation of the references to color in this figure legend, the reader is referred to the Web version of this article.)

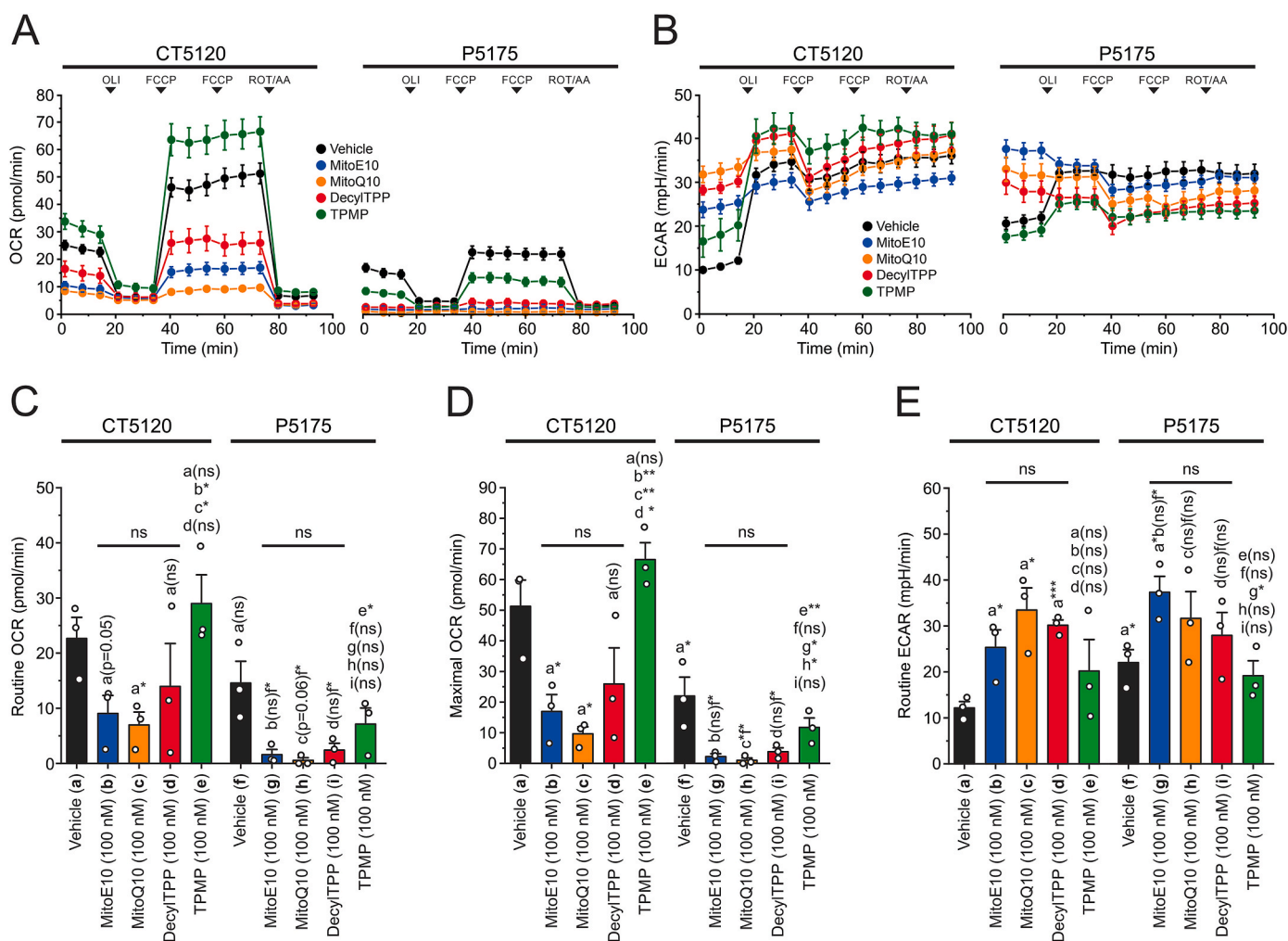


Fig. 4. Effect of MitoE10, MitoQ10, decylTPP and TPMP on oxygen consumption and extracellular acidification rate. PHSFs from a healthy individual (CT5120) and an LS patient (P5175) were cultured for 96 h in the presence of 100 nM MitoE10, MitoQ10, decylTPP and TPMP. Next, oxygen consumption rate (OCR) and extracellular acidification rate (ECAR) were quantified as a function of time. (A) Average OCR trace of CT5120 and P5175 cells. During the recording, various inhibitors were added at the indicated timepoints (arrowheads): oligomycin (OLI), FCCP (2 additions) and a rotenone (ROT) + antimycin A combination (ROT/AA; see Supplemental for details). (B) Same as panel A but now depicting the average ECAR trace. (C) Average routine OCR values (reflecting the basal OCR in the absence of inhibitors). (D) Average maximal OCR values (reflecting the OCR in the presence of OLI and 2 FCCP additions). (E) Average routine ECAR values (reflecting the basal ECAR in the absence of inhibitors). Statistics: the data in this figure was normalized on cell count and represents 3 independent experiments (6 technical replicates each). Statistics was performed using the average value of each independent experiment and significant differences (panel C–D–E) with the indicated conditions (a–i) are marked by: * ($p < 0.05$) and *** ($p < 0.001$); “ns” indicates not significant. In case of borderline significance, numerical p values are presented.

P5175 cells (Fig. 6B; $R = 0.96$; $p < 0.0001$; slope = 2.32 ± 0.068 (SE)). This means that data from either compartment can be used to compare HET-oxidizing ROS levels between conditions. In the vehicle-treated condition, HET-oxidizing ROS levels were higher in P5175 than in CT5120 cells (Fig. 6C and D; gray bars), compatible with the former cells being CI deficient and our previous results [2]. In both cell lines, treatment with 10 nM or 100 nM of MitoE10 decreased and increased ROS levels, respectively (Fig. 6C and D; blue bars), whereas TPMP was without effect (Fig. 6C and D; green bars). This suggests that MitoE10 either acts as an antioxidant (10 nM) or prooxidant (100 nM) in a concentration-dependent manner. In CT5120 cells, MitoQ10 displayed a similar anti/prooxidant effect as MitoE10, whereas in P5175 cells MitoQ10 acted as a prooxidant at both concentrations (Fig. 6C and D; orange bars). Remarkably, decylTPP displayed pro-oxidant properties in CT5120 cells at both concentrations (Fig. 6C; red bars) but antioxidant (10 nM) or prooxidant properties (100 nM) in P5175 cells (Fig. 6D; red bars). For all conditions, HET oxidation was higher in P5175 cells than in CT5120 cells (Supplementary Fig. S6). Of note, short-term treatment with MitoQ10, decylTPP or TPMP (100 nM; 30 min) did not increase HET

oxidation in CT5120 and P5175 cells (Supplementary Figs. S3B–C). This observation, combined with the lack of effect of these treatments on CI levels/activity (Supplementary Fig. S3A), suggests that increased HET oxidation arises from lower CI and/or ETC supercomplex levels. Taken together, these results suggest that MitoE10 and MitoQ10 can display antioxidant or prooxidant effects in a concentration-dependent manner, and that these effects are probably induced by their decylTPP moiety.

3.7. Effect of MitoE10, MitoQ10, decylTPP and TPMP on the membrane fluidity of the mitochondrial inner membrane in isolated rat liver mitochondria

Evidence is accumulating that the lipid composition and physicochemical properties (e.g. fluidity) of the MIM are relevant for ETC (super)complex stability and function [48–51]. Therefore, we determined whether Trolox, MitoE10, MitoQ10, decylTPP and TPMP affected mitochondrial membrane fluidity in isolated rat liver mitochondria. To this end, mitochondria were stained with TMA-DPH to monitor the fluidity in the polar (hydrophobic-hydrophilic) region of the membrane

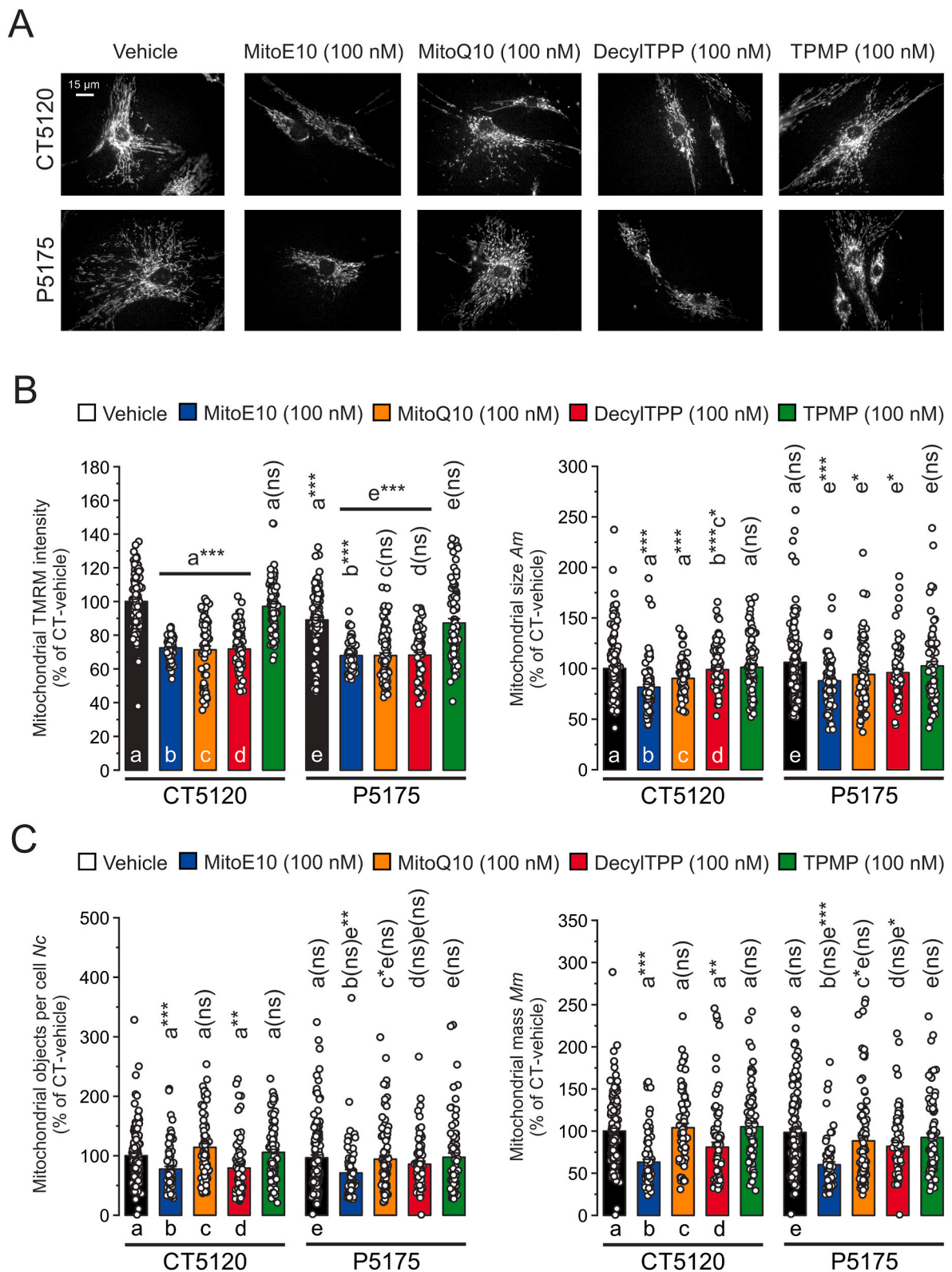


Fig. 5. Effect of MitoE10, MitoQ10, decylTPP and TPMP on mitochondrial TMRM staining intensity and mitochondrial morphology parameters. PHSFs from a healthy individual (CT5120) and an LS patient (P5175) were cultured for 96 h in the presence of MitoE10, MitoQ10, decylTPP and TPMP. (A) Typical live-cell fluorescence microscopy images (contrast-optimized for visualization purposes) of vehicle- and compound-treated PHSFs stained with the fluorescent cation tetramethylrhodamine methyl ester (TMRM). (B) Effect of the compounds on the TMRM fluorescence intensity (left panel) and size (*Am*; right panel) of individual TMRM-positive objects. Data was expressed as percentage of the average value in vehicle-treated CT5120 cells measured on the same day. (C) Same as panel B, but now for the number of TMRM-positive objects per cell (*Nc*; left panel) and mitochondrial mass (*Mm*; right panel). Statistics: The data in panel B–C was obtained in 3 independent experiments for CT5120 (Vehicle: n = 137 cells; MitoE10: n = 77; MitoQ10: n = 74; decylITP: n = 78; TPMP, n = 90) and P5175 (Vehicle: n = 138; MitoE10: n = 74; MitoQ10: n = 87; decylITP: n = 72; TPMP, n = 77). Each symbol reflects an individual cell. Significant differences with the indicated conditions (a–e) are indicated by *(p < 0.05) and ***(p < 0.001); “ns” indicates not significant.

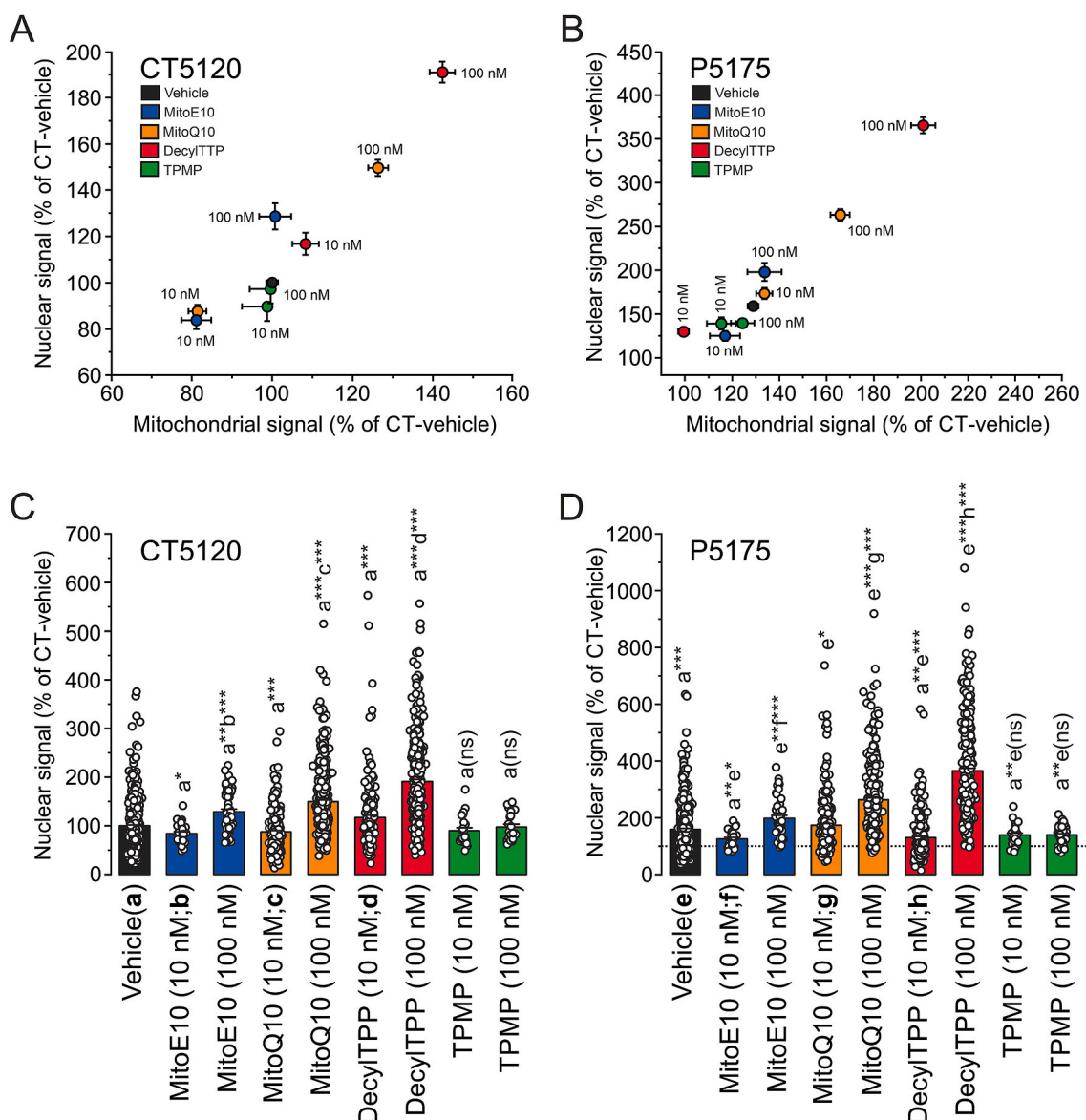


Fig. 6. Effect of MitoE10, MitoQ10, decylTPP and TPMP on hydroethidine oxidation. PHSFs from a healthy individual (CT5120) and an LS patient (P5175) were cultured for 96 h in the presence of 10 or 100 nM MitoE10, MitoQ10, decylTPP and TPMP. (A) Average fluorescence signal of HET oxidation products (CT5120 cells) in a mitochondria-enriched (x-axis) and nuclear (nucleoplasmic; y-axis) region of interest. (B) Same as panel A but now for P5175 cells. (C) Average nuclear signals for the conditions in panel A. (D) Average nuclear signals for the conditions in panel B. The dotted line reflects the signal in vehicle-treated CT5120 cells (condition a in panel C). Statistics: All data in this figure was expressed as a percentage of the average value in vehicle-treated CT5120 cells measured on the same day. Each symbol reflects an individual cell. At least 2 independent experiments were performed for CT5120 (Vehicle: n = 592 cells; 10 nM MitoE10: n = 31; 100 nM MitoE10: n = 57; 10 nM MitoQ10: n = 235; 100 nM MitoQ10: n = 401; 10 nM decylTPP: n = 204; 100 nM decylTPP: n = 368; 10 nM TPMP: n = 23; 100 nM TPMP: n = 21) and P5175 (Vehicle: n = 467; 10 nM MitoE10: n = 28; 100 nM MitoE10: n = 45; 10 nM MitoQ10: n = 250; 100 nM MitoQ10: n = 315; 10 nM decylTPP: n = 277; 100 nM decylTPP: n = 324; 10 nM TPMP: n = 28; 100 nM TPMP, n = 42). Significant differences with the indicated conditions (a–h) are indicated by: * ($p < 0.05$), ** ($p < 0.01$) and *** ($p < 0.001$); “ns” indicates not significant.

bilayer, or DPH to assess the fluidity of the core (hydrophobic region between the two membrane leaflets) of the bilayer [52,53]. An increase in fluorescence polarization of these reporters corresponds to a decrease in membrane fluidity [54]. Incubation with Trolox or TPMP did not affect TMA-DPH polarization (Fig. 7A) and DPH polarization (Fig. 7B), indicating that these molecules do not detectably alter the fluidity of mitochondrial membranes. In contrast, MitoE10, MitoQ10 and decylTPP increased TMA-DPH fluorescence polarization, suggesting that these molecules reduce the fluidity of the polar region of the MIM. In addition, MitoE10 and MitoQ10 increased DPH fluorescence polarization, suggesting that these molecules also reduced membrane fluidity deeper within the MIM. The latter was not observed for decylTPP and TPMP. These results suggest that the decylTPP moiety in principle can lower the

fluidity of the MIM inner leaflet in a concentration-dependent manner. Moreover, it suggests that the headgroups of MitoE10 (i.e. Trolox) and MitoQ10 (i.e. ubiquinone) can reduce membrane fluidity deeper within the MIM.

4. Discussion

This study provides evidence that chronic treatment with MitoE10, MitoQ10 and decylTPP (100 nM; 96 h) reduces the level/activity of CI holocomplexes and ETC supercomplex content in PHSFs, and that the decylTPP moiety is responsible for these phenomena.

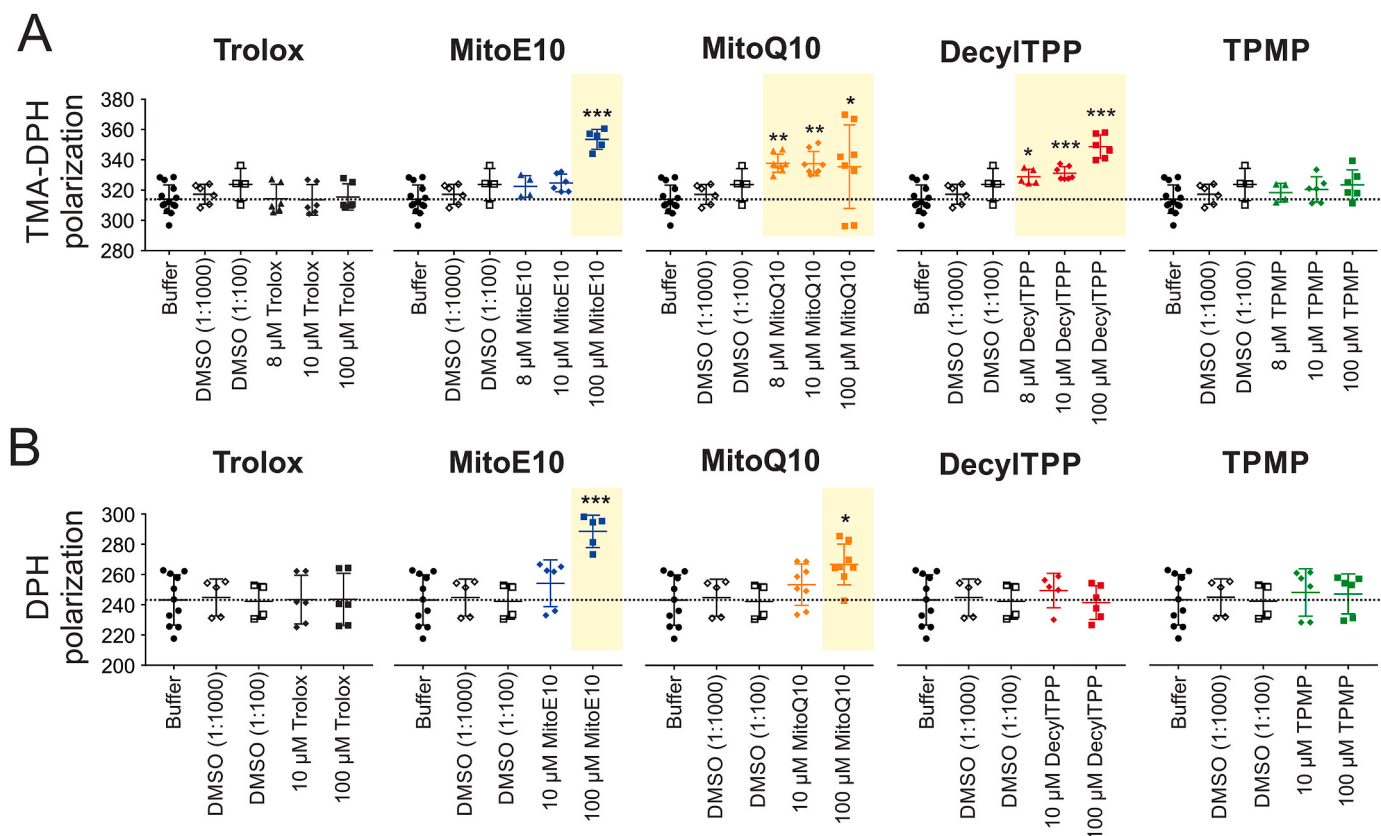


Fig. 7. Effect of Trolox, MitoE10, MitoQ10, decylTPP and TPMP on mitochondrial membrane fluidity. Rat liver mitochondria were freshly isolated and incubated during 2 h with buffer, two dilutions of the solvent (vehicle) DMSO (1:1000, 1:100), or the indicated concentrations of Trolox, MitoE10, MitoQ10, decylTPP or TPMP. (A) Fluorescence polarization of TMA-DPH in the presence of the various compounds. An increase in polarization reflects a reduction in membrane fluidity. (B) Same as panel A but now for DPH polarization. Statistics: Two to six independent experiments were performed for each condition. Individual symbols reflect technical replicates. Significant differences are marked by yellow boxes and by: * ($p < 0.05$), ** ($p < 0.01$) and *** ($p < 0.001$). (For interpretation of the references to color in this figure legend, the reader is referred to the Web version of this article.)

4.1. MitoE10, MitoQ10 and decylTPP reduce ETC supercomplex levels

In the absence of alkylTPP treatment, CT5120 cells contained relatively low levels of the HMW supercomplex (band e) and CI-mon (band a), whereas these signals were not detected in P5175 cells (Fig. 3). Under these conditions, CI and CIII immunoreactivity was primarily associated with ETC supercomplexes in CT5120 and P5175 cells. Treatment with MitoE10, MitoQ10 and decylTPP reduced the level of these supercomplexes and increased “free” CIII-dim levels in CT5120 and P5175 cells. It was previously demonstrated that ETC supercomplexes are not formed when one of their component complexes is missing [36]. Collectively, this suggests that: (1) MitoE10, MitoQ10 and decylTPP decrease ETC supercomplex levels by lowering the levels of CI-mon, (2) CI monomers are destabilized when not incorporated in an ETC supercomplex, and (3) CIII dimers are (more) stable than CI monomers when released from the ETC supercomplex. In case of MitoQ10 it was observed that this molecule also greatly reduced CII holocomplex levels in both cell lines. Since a similar effect was not observed for MitoE10 and decylTPP, it appears that the MitoQ10 “cargo” molecule (ubiquinol) is responsible for lowering CII holocomplex levels. This might be related to the fact that MitoQ10 is redox-cycled to its active antioxidant form (ubiquinol) by CII but not by CI and CIII [22,55]. CI-mediated ROS production is less when it is incorporated in an ETC supercomplex [37]. Indeed, reduced ETC supercomplex levels were paralleled by increased levels of H₂O₂-oxidizing ROS in untreated and vehicle-treated P5175 (which are CI-deficient) relative to CT5120 cells (which are not CI-deficient). Moreover, treatment with MitoE10, MitoQ10 and decylTPP increased these ROS to higher levels in P5175 (displaying

lower CI and supercomplex levels) than in CT5120 cells (displaying higher CI and supercomplex levels). These results agree with previous work demonstrating that H₂O₂ oxidation increases with decreasing CI residual activity and decreasing CI holocomplex levels in LS patient PHSFs [2]. Although effects were only detected at relatively high (μM) concentrations (Fig. 7), our results suggest that the decylTPP moiety can lower the fluidity of the MIM inner leaflet and that the “cargos” of MitoQ10 (ubiquinol) and MitoE10 (Trolox) reduce membrane fluidity deeper within the MIM. Therefore we hypothesize that MitoE10 and MitoQ10 reduce MIM fluidity in a decylTPP-mediated manner, and that this reduction potentially destabilizes the CI holocomplex and/or ETC supercomplexes.

4.2. MitoE10, MitoQ10 and decylTPP impair mitochondrial function

We previously demonstrated that inhibitor-induced CI deficiency stimulates glycolytic flux in CT5120 cells [43]. In this study, it was observed that CT5120 cells displayed a higher OCR and lower ECAR than P5175 cells (Fig. 4). This might suggest that CI-deficient P5175 cells display a more active glycolytic ATP generation to compensate for reduced mitochondrial ATP production [40–42]. MitoE10, MitoQ10 and decylTPP reduced OCR in CT5120 and P5175 cells, with the latter displaying the lowest OCR values. This effect can be explained by the reduced incorporation of CI-mon into ETC supercomplexes, which lowers the level of these supercomplexes [36], thereby impairing mitochondrial oxygen consumption [38]. OCR was reduced to lower levels in P5175 than in CT5120 cells, compatible with the fact that MitoE10, MitoQ10 and decylTPP lowered CI and ETC supercomplex

levels to a greater extent in P5175 than in CT5120 cells. Using P5175 cells, we previously demonstrated that its *NDUFS7* mutation compromises CI assembly and/or stability [56]. In this sense, the greater impact of MitoE10, MitoQ10 and decylTPP might suggest that MIM insertion of MitoE10, MitoQ10 and decylTPP destabilizes CI-mon to a greater extent in P5175 cells than in CT5120 cells. The fact that ECAR was increased by MitoE10, MitoQ10 and decylTPP suggests that glycolytic flux was stimulated in CT5120 and P5175 cells [40]. Increased ECAR can also be caused by enhanced CO₂ production via the TCA cycle [57]. However, we previously demonstrated that mitochondrial NAD(P)H autofluorescence increases with the degree of CI deficiency in a collection of ten CI-deficient patient-derived fibroblasts [58]. In addition, we observed that mitochondrial NAD(P)H autofluorescence is increased in MitoQ10-treated CT5120 and P5175 cells (WJHK, unpublished observation). NADH inhibits all the regulatory enzymes in the TCA cycle, meaning that the degree of TCA cycle inhibition increases with decreasing CI activity. MitoE10, MitoQ10 and decylTPP reduced the levels of CI-mon, ETC supercomplexes and OCR to a large extent, particularly in P5175 cells. Therefore, although we cannot completely rule out involvement of other mechanisms contributing to the increased ECAR, it is less likely that enhanced TCA-mediated CO₂ production is responsible for this increase.

5. Conclusions

Our results suggest a potential mechanism in which MIM insertion of MitoE10/MitoQ10/decylTPP destabilizes CI and/or ETC

supercomplexes, thereby lowering overall CI/ETC activity, mitochondrial oxygen consumption and ATP generation (Fig. 8). Although not investigated in this study, ETC supercomplex destabilization might be (co)mediated by MitoE10/MitoQ10/decylTPP impacting on the mitochondrial MIM lipid cardiolipin, known to play a role in ETC supercomplex stability [59]. Loss of ETC supercomplexes was paralleled by mitochondrial fragmentation and increased ROS levels, compatible with previous studies [37,44]. We hypothesize that CI/ETC deficiency and ensuing mitochondrial dysfunction induces a compensatory activation of glycolytic ATP generation to prevent energy crisis and cell death (Fig. 8). The overall cellular effects of mitochondria-targeted Trolox (*i.e.* MitoE10) in this study greatly differed from those of “non-targeted” Trolox [23–25]. This likely relates to our current finding that the cellular effects of MitoE10 (and MitoQ10) are primarily due to their decylTPP mitochondria-targeting moiety. The latter is highly relevant since decylTPP-mediated targeting has been applied for a wide variety of “cargos” including (fluorescent) reporter molecules, therapeutics, nanoparticles, polymersomes and MRI contrast agents [16,31,60,61]. It is not straightforward to directly extrapolate our cell data to animal/human studies with alkylTPP compounds. This is due the fact that the (intra)cellular and mitochondrial concentrations of these compounds are generally unknown in animal/human models and that mitochondria-targeting group itself is not always included in control experiments to demonstrate that its attached cargo molecule displays specific effects. We advocate that studies employing alkylTPP-mediated mitochondrial targeting strategies should routinely include control experiments with the corresponding alkylTPP moiety.

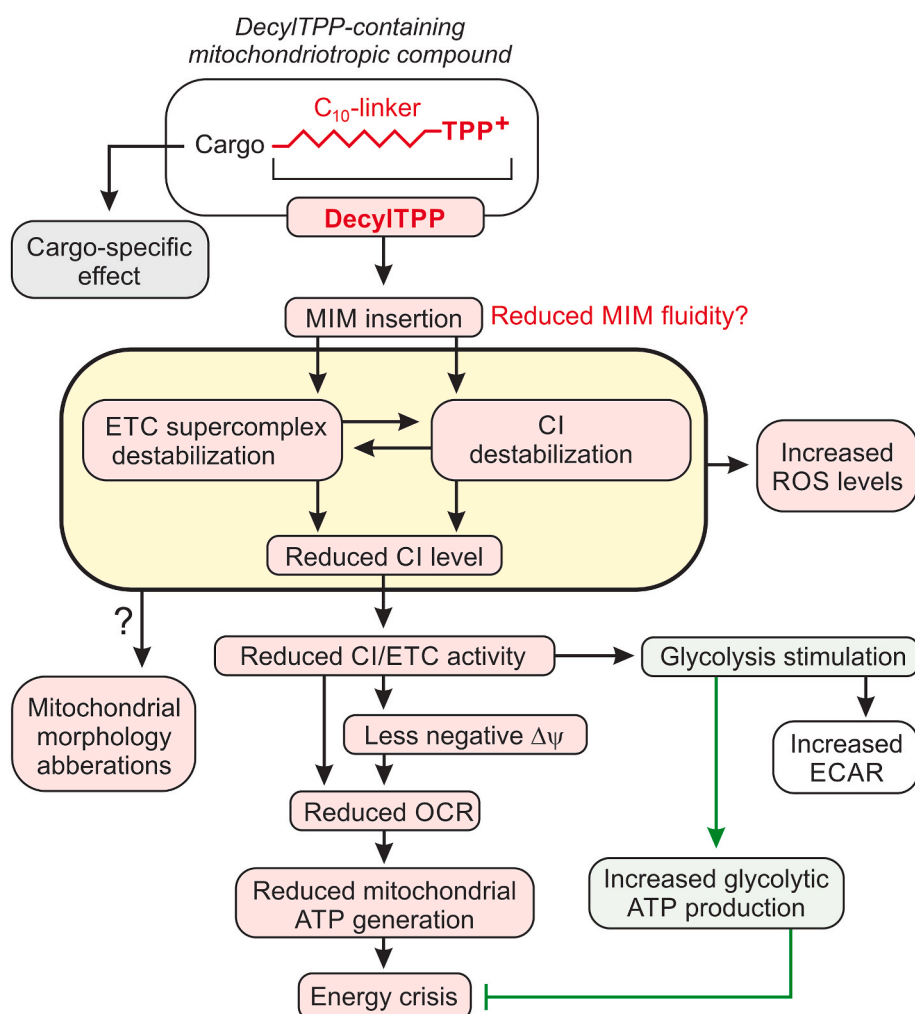


Fig. 8. Proposed chain-of-events for decylTPP-induced mitochondrial dysfunction. DecylTPP-containing molecules contain a cargo moiety and a mitochondria-targeting moiety (decylTPP). Paralleled by cargo-specific effects, MIM insertion of the decylTPP moiety destabilizes mitochondrial complex (CI) and ETC supercomplexes (or *vice versa*), potentially by reducing MIM fluidity. As a consequence, the level and activity of the CI holocomplex is reduced, $\Delta\psi$ is depolarized, ETC-mediated ATP generation is impaired, mitochondrial fragmentation is induced and ROS levels are increased. To prevent energy crisis, glycolytic ATP generation is stimulated to prevent energy crisis and maintain cell viability. Abbreviations: $\Delta\psi$ mitochondrial membrane potential; CI, complex I; ECAR, extracellular acidification rate; ETC, electron transport chain; MIM, mitochondrial inner membrane; OCR, oxygen consumption rate; ROS, reactive oxygen species.

Author contributions

Experiments with isolated mitochondria (CE, HZ); Crystal violet analysis (SEvEdV, JW); Seahorse measurements (EPB, LG, NPR); BN-PAGE (EPB; SEvEdV; EvdW; MvdW); TMRM experiments (SEvEdV, EvdW); ROS measurements (EvdW, JW, FD); Data analysis (EPB, CE, LG, EvdW, JW, FD, WJHK); Manuscript writing (EPB, CE, JAMS, RJR, PHGMW, MJWAH, HZ, WJHK); Overall supervision of research (WJHK).

Data availability

Source data and materials are available from the corresponding author upon reasonable request. All other data is presented in the main manuscript and Supplement. This study includes no data deposited in external repositories.

FUNDING

This work was supported by the CSBR (Centres for Systems Biology Research) initiative from the Netherlands Organisation for Scientific Research (NWO; No: CSBR09/013V), a PM-Rare (Priority Medicines Rare disorders and orphan diseases) grant from ZON-MW (Netherlands Organization for Health Research and Development-Medical Sciences, No: 40-41900-98-033), the Energy4All foundation (www.energy4all.eu), the TIM foundation (www.timfoundation.nl) and an equipment grant of NWO (Netherlands Organization for Scientific Research, No: 911-02-008).

Declaration of competing interest

JAMS is the founder and CEO of Khondrion B.V. (Nijmegen, The Netherlands). WJHK is a scientific advisor of Khondrion B.V. This SME had no involvement in the data collection, analysis and interpretation, writing of the manuscript, and in the decision to submit the manuscript for publication.

Acknowledgements

We thank Dr. A. de Jong (Dept. of Biochemistry, Radboudumc) for assistance with ROS measurements. We also are grateful to Drs. M.P. Murphy and A.M. James (MRC Mitochondrial Biology Unit, University of Cambridge, UK) for providing MitoE10/MitoQ10 and insightful discussions.

Appendix A. Supplementary data

Supplementary data to this article can be found online at <https://doi.org/10.1016/j.freeradbiomed.2022.06.011>.

References

- [1] W.J.H. Koopman, P.H.G.M. Willems, J.A.M. Smeitink, Monogenic mitochondrial disorders, *N. Engl. J. Med.* 366 (2012) 1132–1141.
- [2] S. Verkaar, W.J.H. Koopman, L.G.J. Nijtmans, L.W.P.J. van den Heuvel, J.A. M. Smeitink, P.H.G.M. Willems, Superoxide activity is inversely related to complex I activity in inherited complex I deficiency, *Biochim. Biophys. Acta* 1772 (2007) 373–381.
- [3] H. Salmi, J.V. Leonard, S. Rahman, R. Lepatto, Plasma thiol status is altered in children with mitochondrial diseases, *Scand. J. Clin. Lab. Invest.* 72 (2012) 152–157.
- [4] A.M. Voets, P.J. Lindsey, S.J. Vanherle, E.D. Timmer, J.J. Esseling, W.J. H. Koopman, P.H.G.M. Willems, G.C. Schoonderwoerd, D. De Groote, B.T. Poll-The, I.F.M. de Co, H.J.M. Smeets, Patient-derived fibroblasts indicate oxidative stress status and may justify antioxidant therapy in OXPHOS disorders, *Biochim. Biophys. Acta* 1817 (2012) 1971–1978.
- [5] A.M. Voets, M. Huigsloot, P.J. Lindsey, A.M. Leenders, W.J.H. Koopman, P.H.G.M. Willems, R.J. Rodenburg, J.A. Smeitink, H.J. Smeets, Transcriptional changes in OXPHOS complex I deficiency are related to anti-oxidant pathways and could explain the disturbed calcium homeostasis, *Biochim. Biophys. Acta* 1822 (2012) 1161–1168.
- [6] R. Goldschmidt, P.M. Arce, O.M. Khmour, V.C. Collin, S. Dey, J. Jaruvangsanti, D. M. Fash, S.M. Hecht, Effects of cytoprotective antioxidants on lymphocytes from representative mitochondrial neurodegenerative diseases, *Bioorg. Med. Chem.* 21 (2013) 969–978.
- [7] P.E. Hart, R. Lodi, B. Rajagopalan, J.L. Bradley, J.G. Grilley, C. Turner, A. M. Blamire, D. Manners, P. Styles, A.H. Schapira, J.M. Cooper, Antioxidant treatment of patients with Friedreich ataxia: four-year follow-up, *Arch. Neurol.* 62 (2005) 621–626.
- [8] D. Martinelli, M. Catteruccia, F. Piemonte, A. Pastore, G. Tozzi, C. Dionisi-Vici, G. Pontrelli, T. Corsetti, S. Livadiotti, V. Kheifets, A. Hinman, W.D. Schrader, M. Thoolen, M.B. Klein, E. Bertini, G. Miller, EPI-743 reverses the progression of the pediatric mitochondrial disease - genetically defined Leigh Syndrome, *Mol. Genet. Metabol.* 107 (2012) 383–388.
- [9] G. Pfeffer, R. Horvath, T. Klopstock, V.K. Mootha, A. Suomalainen, S. Koene, M. Hirano, M. Zeviani, L.A. Bindoff, P. Yu-Wai-Man, M. Hanna, V. Carelli, R. McFarland, K. Majamaa, D.M. Turnbull, J. Smeitink, P.F. Chinnery, New treatments for mitochondrial disease - no time to drop our standards, *Nat. Rev. Neurol.* 9 (2013) 474–481.
- [10] G. Bjelakovic, D. Nikolova, L.L. Gluud, R.G. Simonetti, C. Gluud, Mortality in randomized trials of antioxidant supplements for primary and secondary prevention: systematic review and meta-analysis, *JAMA* 297 (2007) 842–857.
- [11] D. Heyland, J. Muscedere, P.E. Wischmeyer, D. Cook, G. Jones, M. Albert, G. Elge, M.M. Berger, A.G. Day, Canadian Critical Care Trials Group, A randomized trial of glutamine and antioxidants in critically ill patients, *N. Engl. J. Med.* 368 (2013) 1489–1497.
- [12] H.H. Schmidt, R. Stocker, C. Vollbracht, G. Paulsen, D. Riley, A. Daiver, A. Cuadrado, Antioxidants in translational medicine, *Antioxidants Redox Signal.* 23 (2015) 1130–1143.
- [13] B. Halliwell, M.C. Gutteridge, *Free Radicals in Biology and Medicine*, Oxford University Press, Inc., New York, USA, 2007.
- [14] M.P. Murphy, R.A.J. Smith, Targeting antioxidants to mitochondria by conjugation to lipophilic cations, *Annu. Rev. Pharmacol. Toxicol.* 47 (2007) 629–656.
- [15] A. Bast, G.R.R.M. Haenen, Ten misconceptions about antioxidants, *Trends Pharmacol. Sci.* 34 (2013) 430–436.
- [16] N. Apostolova, V.M. Victor, Molecular strategies for targeting antioxidants to mitochondria: therapeutic implications, *Antioxidants Redox Signal.* 22 (2015) 686–729.
- [17] V.P. Skulachev, How to clean the dirtiest place in the cell: cationic antioxidants as intramitochondrial ROS scavengers, *IUBMB Life* 57 (2005) 305–310.
- [18] M.F. Ross, T.A. Prime, I. Abakumova, A.M. James, C.M. Porteous, R.A.J. Smith, M. P. Murphy, Rapid and extensive uptake and activation of hydrophobic triphenylphosphonium cations within cells, *Biochem. J.* 411 (2008) 633–645.
- [19] C.C. Kang, W.C. Huang, C.W. Kouh, Z.F. Wang, C.C. Cho, C.C. Chang, C.L. Wang, T. C. Chang, J. Seemann, L.J.S. Huang, Chemical principle for a novel fluorescent probe with high cancer-targeting selectivity and sensitivity, *Integr. Biol.* 5 (2013) 1217–1288.
- [20] L.S. Khailova, P.A. Nazarov, N.V. Sumbatyan, G.A. Korshunova, T.I. Rokitskaya, V. I. Dedukhova, Y.N. Antonenko, V.P. Skulachev, Uncoupling and toxic action of alkylphenylphosphonium cations on mitochondria and the bacterium *Bacillus subtilis* as a function of alkyl chain length, *Biochemistry (Mosc.)* 80 (2015), 15891597.
- [21] J. Asin-Cayuela, A.R.B. Manas, A.M. James, R.A.J. Smith, M.P. Murphy, Fine-tuning the hydrophobicity of a mitochondria-targeted antioxidant, *FEBS Lett.* 571 (2004) 9–16.
- [22] A.M. James, M.S. Sharpley, A.R.B. Manas, F.E. Frerman, J. Hirst, R.A.J. Smith, M. P. Murphy, Interaction of the mitochondria-targeted antioxidant MitoQ with phospholipid bilayers and ubiquinone oxidoreductases, *J. Biol. Chem.* 282 (2007) 14708–14718.
- [23] W.J.H. Koopman, S. Verkaar, S.E. van Emst-de Vries, S. Grefte, J.A.M. Smeitink, L. G.J. Nijtmans, P.H.G.M. Willems, Mitigation of NADH:ubiquinone oxidoreductase deficiency by chronic Trolox treatment, *Biochim. Biophys. Acta* 1777 (2008) 853–859.
- [24] R.H. Triepels, L.P. van den Heuvel, J.L. Loeffen, C.A. Buskens, R.J. Smeets, M. E. Rubio Gosalbo, S.M. Budde, E.C. Mariman, F.A. Wijburg, P.G. Barth, J. M. Trijbels, J.A.M. Smeitink, Leigh syndrome associated with a mutation in the NDUFS7 (PSST) nuclear encoded subunit of complex I, *Ann. Neurol.* 45 (1999) 787–790.
- [25] F. Distelmaier, F. Valsecchi, M. Forkink, S. van Emst-de Vries, H. Swarts, R. Rodenburg, E. Verwiel, J. Smeitink, P.H.G.M. Willems, W.J.H. Koopman, Trolox-sensitive ROS regulate mitochondrial morphology, oxidative phosphorylation and cytosolic calcium handling in healthy cells, *Antioxidants Redox Signal.* 17 (2012) 1657–1669.
- [26] H.M. Cochemé, G.F. Kelso, A.M. James, M.F. Ross, J. Trnka, T. Mahendiran, J. Asin-Cayuela, F.H. Blaikie, A.R. Manas, C.M. Porteous, V.J. Adlam, R.A. Smith, M.P. Murphy, Mitochondrial targeting of quinones: therapeutic implications, *Mitochondrion* 7S (2007) S94–S102.
- [27] J. Teixeira, P. Soares, S. Benefito, A. Gaspar, J. Garrido, M.P. Murphy, F. Borges, Rational discovery and development of a mitochondria-targeted antioxidant based on cinnamic acid scaffold, *Free Radic. Res.* 46 (2012) 600–611.
- [28] J. Trnka, M. Elkalaf, M. Anděl, Lipophilic triphenylphosphonium cations inhibit mitochondrial electron transport chain and induce mitochondrial proton leak, *PLoS One* 10 (2015), e0121837.
- [29] J. Truksa, L.F. Dong, J. Rohlena, J. Stursa, M. Vondrusova, J. Goodwin, M. Nguyen, K. Kluckova, Z. Rychtarčíková, S. Lettlova, J. Spacilova, M. Stapelberg, M. Zoratti, J. Neuzil, Mitochondrially targeted vitamin E succinate modulates expression of

- mitochondrial DNA transcripts and mitochondrial biogenesis, *Antioxidants Redox Signal.* 22 (2015) 883–900.
- [30] K.L. Pokrzywinski, T.G. Biel, D. Kryndushkin, V.A. Rao, Therapeutic targeting of the mitochondria initiates excessive superoxide production and mitochondrial depolarization causing decreased mtDNA integrity, *PLoS One* 11 (2016), e0168283.
- [31] J. Zielonka, J. Joseph, A. Sikora, M. Hardy, O. Ouari, J. Vasquez-Vivar, G. Cheng, M. Lopez, B. Kalyanaraman, Mitochondria-targeted triphenylphosphonium-based compounds: syntheses, mechanisms of action, and therapeutic and diagnostic applications, *Chem. Rev.* 117 (2017) 10043–10120.
- [32] E.M. Gottwald, M. Duss, M. Bugarski, D. Haenni, C.D. Schuh, E.M. Landau, A. M. Hall, The targeted anti-oxidant MitoQ causes mitochondrial swelling and depolarization in kidney tissue, *Phys. Rep.* 6 (2018), e13667.
- [33] J.A. Armstrong, N.J. Cash, J.C. Morton, A.V. Tepikin, R. Sutton, D.N. Criddle, Mitochondrial targeting of antioxidants alters pancreatic acinar cell bioenergetics and determines cell fate, *Int. J. Mol. Sci.* 20 (2019) 1700.
- [34] W.J.H. Koopman, S. Verkaart, H.J. Visch, F.H. van der Westhuizen, M.P. Murphy, L.W. van den Heuvel, J.A. Smeitink, P.H.G.M. Willems, Inhibition of complex I of the electron transport chain causes oxygen radical-mediated mitochondrial outgrowth, *Am. J. Physiol. Cell Physiol.* 288 (2005) C1440–C1450.
- [35] H. Schägger, K. Pfeiffer, Supercomplexes in the respiratory chains of yeast and mammalian mitochondria, *EMBO J.* 19 (2000) 1777–1783.
- [36] R. Acín-Pérez, P. Fernández-Silva, M.L. Peleato, A. Pérez-Martos, J.A. Enriquez, Respiratory active mitochondrial supercomplexes, *Mol. Cell* 32 (2008) 529–539.
- [37] E. Maranzana, G. Barbero, A.I. Falasca, G. Lenaz, M.L. Genova, Mitochondrial respiratory supercomplex association limits production of reactive oxygen species from complex I, *Antioxidants Redox Signal.* 19 (2013) 1469–1480.
- [38] I. Lopez-Fabuel, J. Le Douce, A. Logan, A.M. James, G. Bonvento, M.P. Murphy, A. Almeida, J.P. Bolaños, Complex I assembly into supercomplexes determines differential mitochondrial ROS production in neurons and astrocytes, *Proc. Natl. Acad. Sci. U.S.A.* 113 (2016) 13063–13068.
- [39] I. Vercellino, L.A. Sazanov, Structure and assembly of the mammalian mitochondrial supercomplex CIII₂CIV, *Nature* 598 (2021) 364–367.
- [40] A.S. Divakaruni, A. Paradise, D.A. Ferrick, A.N. Murphy, M. Jastroch, Analysis and interpretation of microplate-based oxygen consumption and pH data, *Methods Enzymol.* 547 (2014) 309–354.
- [41] D.C. Liemburg-Apers, T.J.J. Schirris, F.G.M. Russel, P.H.G.M. Willems, W.J. H. Koopman, Mitochondrial dysfunction triggers a rapid compensatory increase in steady-state glucose flux, *Biophys. J.* 109 (2015) 1372–1386.
- [42] D.C. Liemburg-Apers, J.A.L. Wagenaars, P.H.G.M. Willems, W.J.H. Koopman, Acute inhibition of mitochondrial complex I and III triggers LKB1-, AMPK-, and SIRT2-dependent stimulation of GLUT1 activity, *J. Cell Sci.* 129 (2016) 4411–4423.
- [43] F. Distelmaier, F. Valsecchi, D.C. Liemburg-Apers, M. Lebedzinska, R. J. Rodenburg, S. Heil, J. Keijer, J. Fransen, H. Imamura, K. Danhauser, A. Seibt, B. Viollet, F. Gellerich, J.A.M. Smeitink, M.R. Wieckowski, P.H.G.M. Willems, W.J. H. Koopman, Mitochondrial dysfunction in primary human fibroblasts triggers an adaptive cell survival program that requires AMPK- α , *Biochim. Biophys. Acta* 1852 (2015) 529–540.
- [44] V. Tomková, C. Sandoval-Acuña, N. Torrealba, J. Truksa, Mitochondrial fragmentation, elevated mitochondrial superoxide and respiratory supercomplexes disassembly is connected with the tamoxifen-resistant phenotype of breast cancer cells, *Free Radic. Biol. Med.* 143 (2019) 510–521.
- [45] F. Distelmaier, W.J.H. Koopman, L.W. van den Heuvel, R.J. Rodenburg, E. Mayatepek, P.H.G.M. Willems, J.A.M. Smeitink, Mitochondrial complex I deficiency: from organelle dysfunction to clinical disease, *Brain* 132 (2009) 833–842.
- [46] E.F. Iannetti, J.A.M. Smeitink, P.H.G.M. Willems, J. Beyrath, W.J.H. Koopman, Rescue from galactose-induced death of Leigh Syndrome patient cells by pyruvate and NAD⁺, *Cell Death Dis.* 9 (2018) 1135.
- [47] S. Grefte, W.J.H. Koopman, Live-cell assessment of reactive oxygen species levels using dihydroethidine, *Methods Mol. Biol.* 2276 (2021) 291–299.
- [48] C.U. Mårtensson, K.N. Doan, T. Becker, Effects of lipids on mitochondrial functions, *Biochim. Biophys. Acta. Mol. Cell. Biol. Lipids.* (2017) 102–113, 1862.
- [49] I. Budin, T. de Rond, Y. Chen, L.J.G. Chan, C.J. Petzold, J.D. Keasling, Viscous control of cellular respiration by membrane lipid composition, *Science* 362 (2018) 1186–1189.
- [50] P. Hernansanz-Agustín, C. Choya-Foces, S. Carregal-Romero, E. Ramos, T. Oliva, T. Villa-Piña, L. Moreno, A. Izquierdo-Álvarez, J.D. Cabrera-García, A. Cortés, A. V. Lechuga-Vieco, P. Jadiya, E. Navarro, E. Parada, A. Palomino-Antolín, D. Tello, R. Acín-Pérez, J.C. Rodríguez-Aguilera, P. Navas, Á. Cogolludo, I. López-Montero, Á. Martínez-Del-Pozo, J. Egea, M.G. López, J.W. Elrod, J. Ruiz-Cabello, A. Bogdanova, J.A. Enriquez, A. Martínez-Ruiz, Na⁺ controls hypoxic signaling by the mitochondrial respiratory chain, *Nature* 586 (2020) 287–291.
- [51] M. Schlame, Protein crowding in the inner mitochondrial membrane, *Biochim. Biophys. Acta Bioenerg.* 1862 (2021), 148305.
- [52] J. Grebowski, A. Krokosz, M. Puchala, Membrane fluidity and activity of membrane ATPases in human erythrocytes under the influence of polyhydroxylated fullerene, *Biochim. Biophys. Acta* 1828 (2013) 241–248.
- [53] C. Einer, S. Hohenester, R. Wimmer, L. Wottke, R. Artmann, S. Schulz, C. Gosmann, A. Simmons, C. Leitzinger, C. Eberhagen, S. Borchard, S. Schmitt, S.M. Hauck, C. von Toerne, M. Jastroch, E. Walheim, C. Rust, A.L. Gerbes, B. Popper, D. Mayr, M. Schnurr, A.M. Vollmar, G. Denk, H. Zischka, Mitochondrial adaptation in steatotic mice, *Mitochondrion* 40 (2018) 1–12.
- [54] M. Shinitzky, Y. Barenholz, Fluidity parameters of lipid regions determined by fluorescence polarization, *Biochim. Biophys. Acta* 515 (1978) 367–394.
- [55] A.M. James, H.M. Cochemé, R.A.J. Smith, M.P. Murphy, Interactions of mitochondria-targeted and untargeted ubiquinones with the mitochondrial respiratory chain and reactive oxygen species, *J. Biol. Chem.* 280 (2005) 21295–21312.
- [56] C. Ugalde, R.J.R.J. Janssen, L.P. van den Heuvel, J.A.M. Smeitink, L.G.J. Nijtmans, Differences in assembly or stability of complex I and other mitochondrial complexes in inherited complex I deficiency, *Hum. Mol. Genet.* 13 (2004) 659–667.
- [57] C.A. Schmid, K.H. Fisher-Wellman, P.D. Neuffer, From OCR and ECAR to energy: perspectives on the design and interpretation of bioenergetics studies, *J. Biol. Chem.* 297 (2021), 101140.
- [58] S. Verkaart, W.J.H. Koopman, J. Cheek, S.E. van Emst-de Vries, L.W. van den Heuvel, J.A. Smeitink, P.H. Willems, Mitochondrial and cytosolic thiol redox state are not detectably altered in isolated human NADH:ubiquinone oxidoreductase deficiency, *Biochim. Biophys. Acta* 1772 (2007) 1041–1051.
- [59] L. Böttinger, S.E. Horvath, T. Kleinschroth, C. Hunte, G. Daum, N. Pfanner, T. Becker, Phosphatidylethanolamine and cardiolipin differentially affect the stability of mitochondrial respiratory chain supercomplexes, *J. Mol. Biol.* 423 (2012) 677–686.
- [60] B.A. Feniouk, V.P. Skulachev, Cellular and molecular mechanisms of action of mitochondria-targeted antioxidants, *Curr. Aging Sci.* 10 (2017) 41–48.
- [61] M. Momcilovic, A. Jones, S.T. Bailey, C.M. Waldmann, R. Li, J.T. Lee, G. Abdelhady, A. Gomez, T. Holloway, E. Schmid, D. Stout, M.C. Fishbein, L. Stiles, D.V. Dabir, S.M. Dubinett, H. Christofk, O. Shirihai, C.M. Koehler, S. Sadeghi, D. B. Shackelford, *In vivo* imaging of mitochondrial membrane potential in non-small lung cancer, *Nature* 575 (2019) 380–384.
- [62] R.A.J. Smith, C.M. Porteous, C.V. Coulter, M.P. Murphy, Selective targeting of an antioxidant to mitochondria, *Eur. J. Biochem.* 263 (1999) 709–716.
- [63] R.A.J. Smith, C.M. Porteous, A.M. Gane, M.P. Murphy, Delivery of bioactive molecules to mitochondria *in vivo*, *Proc. Natl. Acad. Sci. USA* 100 (2003) 5407–5412.
- [64] P.G. Finichiu, A.M. James, L. Larsen, R.A.J. Smith, M.P. Murphy, Mitochondrial accumulation of a lipophilic cation conjugated to an ionisable group depends on membrane potential, pH gradient and pK_a; implications for the design of mitochondrial probes and therapies, *J. Bioenerg. Biomembr.* 45 (2013) 165–173.
- [65] V.J.A. Jameson, H.M. Cochemé, A. Logan, L.R. Hanton, R.A.J. Smith, M.P. Murphy, Synthesis of triphenylphosphonium vitamin E derivatives as mitochondria-targeted antioxidants, *Tetrahedron* 71 (2015) 8444–8453.
- [66] E. Niki, K. Abe, Chapter 1: vitamin E: structure, properties and functions, in: E. Niki (Ed.), *Vitamin E: Chemistry and Nutritional Benefits*, The Royal Society of Chemistry, Cambridge, UK, 2019, pp. 1–11.
- [67] L. Socrier, M. Rosselin, A.M. Gomez Giraldo, B. Chantemargue, F. Di Meo, P. Trouillas, G. Durand, S. Morandat, Nitro-Trolox conjugate as an inhibitor of lipid oxidation: towards synergistic antioxidant effects, *Biochim. Biophys. Acta* 1861 (2019) 1489–1501.